COBEM 2023 27TH INTERNATIONAL CONGRESS OF MECHANICAL ENGENEERING

ABCM Brazilian Society of Mechanical Sciences and Engineering
27th ABCM International Congress of Mechanical Engineering
December 04-08, 2023, Florianópolis-SC, Brazil

COB-2023-0618
INFLUENCE OF CURVATURE ON RESIDUAL STRESS MEASUREMENT BY X-RAY DIFFRACTION AT THE GEAR TOOTH ROOT

João Pedro Vieira
Competence Center in Manufaturing – CCM-ITA
Praça Marechal Eduardo Gomes, 50, CEP 12228-900 – São José dos Campos - SP
joao.vieira@ccm-ita.org.br

Matheus Monteiro de Siqueira Santos
Instituto Federal de Educação, Ciência e Tecnologia de São Paulo – IFSP
Rodovia Presidente Dutra, km 145, CEP 12223-201 – São José dos Campos - SP
monteiro.santos@aluno.ifsp.edu.br

Tiago Cristofer Aguzzoli Colombo
Faculdade de Tecnologia de São José dos Campos – FATEC
Avenida Cesare Mansueto Giulio Lattes, 1350, CEP 12247-014 – São José dos Campos - SP
tiago.colombo@fatec.sp.gov.br

Ronnie Rodrigo Rego
Competence Center in Manufaturing – CCM-ITA
Praça Marechal Eduardo Gomes, 50, CEP 12228-900 – São José dos Campos - SP
ronnie@ita.br

Abstract. *The root area of the gear tooth geometry is an important site for the accurate assessment of gear condition, especially when considering tooth bending fatigue failure, as the maximum tensile stresses during operation are developed at the root radius. Due to its small diameter, a strong influence of curvature is expected on the stress values obtained, altering their accuracy and precision. In this regard, it is of interest to check whether residual stress measurements are valid at the root region and investigate to what extent they are affected by its curvature, which is the objective of this study. The procedure was carried out using the cosα X-ray diffraction technique on a controlled geometry stress relieved ASTM A36 block on which grooves with varying diameters were indented, as well as evaluation on case hardened steel alloy gear teeth. Residual stress measurements for the machined specimen indicated adequate accuracy for curved surfaces with diameters from 6 to 10 times larger than that of the equipment's collimator, especially in the axial direction. Measurements on a curved groove with diameter only 3 times larger than the collimator's showed significant curvature influence on the circumferential direction, indicated by the high disparity of the stress values obtained when compared to those of the other channels. The teeth roots of the ITA geometry gear were not affected by curvature influence despite their small dimensions, generating precise results for both directions. This behavior is likely due to X-rays being cast onto regions of the tooth root other than that with the smallest radius. Considering the importance of this specific area for evaluation of tooth bending fatigue, modifications are needed and proposed to the standard measurement technique utilizing the cosα X-ray diffraction method at the root region.*

Keywords: *residual stress, X-ray diffraction, gear tooth root*

1. INTRODUCTION

The most common failure mode in gears is tooth bending fatigue (Alban, 1985). In this situation, a crack is originated at the tooth root on the side under tensile stress and is propagated through each cycle until the critical point is reached, when the tooth, weakened by the crack, can no longer withstand the load and breaks. Since fatigue failure cracks in gears are mostly nucleated at the surface (Kramberger *et al.*, 2004), it is essential to ensure adequate surface integrity to increase their fatigue life.

In addition to aspects such as hardness and roughness, residual stress has a significant influence on crack nucleation and propagation behavior in transmission components (James *et al.*, 2007). Tensile stresses accelerate the occurrences of failure, while compressive ones suppress them by mitigating crack development. Using a simplified analysis based on the superposition principle, this behavior can be attributed to the reduction of effective stress during operation (Nelson, 1982).

Considering the great relevance of the failures that occur at the tooth root and the influence of residual stresses on gear fatigue life, it is important that their measurement is accurate and repeatable. Among the different ways of evaluating residual stress, nondestructive methods based on X-ray diffraction have been increasingly used, as they are able to determine the state of stresses on the surface quickly and with good reliability. The recent development of portable, simple to operate and commercially viable techniques utilizing this principle, especially the cosα method, has further enhanced the use of X-ray diffraction for that purpose in recent years (Peterson *et al.*, 2017; Tanaka, 2018).

Once applied to measurements at the gear tooth root, however, these methods bring certain challenges. The geometry of the root region, due to its high curvature, causes the need for correction of the obtained values, since there is disparity between the actual stresses present on the analyzed location and the measured ones. When non-flat components are measured using X-ray diffraction, errors are introduced in the values obtained due to displacement of the diffracted rays. Considering a cylindrical surface, in a simplified manner, as a sum of planes tilted at different angles, each of them induces error by displacing the ray diffracted on it. The resultant X-ray, then, is detected at a position that does not correspond to the diffraction angle that would happen on a flat surface with the same residual stress state. This deviation increases as the curvature diameter decreases and, since the residual stress measurements depend directly on the diffraction angle, they will not accurately portray the real stress present at the region.

Oguri *et al.* have performed a series of experiments in order to correct the errors associated with residual stress measurements on curved surfaces, both cylindrical and spherical, using the $\sin^2\psi$ and cosα methods. In 2017, the researchers analyzed the error introduced on measurements performed on convex cylindrical surfaces utilizing the cosα technique. It was found that the values measured are less compressive than the actual stresses at the region examined, but that the errors can be disregarded if the diameter of the specimen's curvature is smaller than a third of the equipment's collimator diameter. Furthermore, axial stresses measurements (along the cylindrical specimens' length) were significantly more accurate than circumferential ones (around their perimeter), and the validity of the shear residual stresses calculated was considered dubious. It was assumed that the radial residual stress was null.

The objectives of the present study are to check whether the cosα X-ray diffraction technique generates valid results of residual stress at the tooth root, as well as to investigate the extent of the influence of curvature on the precision and accuracy of the values obtained. For this, two lines of measuring experiments were considered: on a steel specimen with indented grooves of different dimensions, and on gear teeth compatible with real analysis procedures.

2. MATERIALS AND METHODS

A Pulstec μ-X360s device was employed to conduct residual stress measurements on an ASTM A36 steel specimen by X-ray diffraction using the cosα method. Equipment precision was confirmed by measuring the same spot multiple times without movement of the block or the device. Teeth from a case hardened AISI 4320 gear of ITA geometry also had their stress state measured at the root area, providing a correlation to practical conditions. A ferritic B.C.C. structure was considered in both cases. The most relevant equipment parameters for the analyses are shown on Tab. 1.

Table 1. Equipment parameters for residual stress measurement via the cosα method.

Parameter	Value
Alpha angle offset	0.0°
Collimator diameter	1.0 mm
Diffraction plane	{211}
Diffraction angle	156.396°
Interplanar spacing	1.170 Å
K-alpha X-ray wavelength	2.29093 Å
Lattice constant	2.8664 Å
Peak analysis method	Lorentz fitting
Pitch	100 μm
Poisson's ratio	0.280
Sample distance (analysis)	52.187 mm
Sample distance (monitor)	51.000 mm
Valid range of alpha angle	18.0° to 90.0°
X-ray incidence angle	35.0°
X-ray irradiation time	30 s
X-ray tube current	1.50 mA
X-ray tube voltage	30.00 kV
Young's modulus	224.000 GPa

2.1 Specimen analysis

A block of ASTM A36 steel with dimensions 200x150x16.2 mm, as shown in Fig. 1, was milled, ground, and afterwards underwent a stress relief heat treatment. This process was done at a soaking temperature of 650 °C for one hour using a heating rate of 400 °C/h, with the specimen then being left to cool inside the furnace, as suggested by studies of stress relief treatment for low carbon steel alloys such as A36 (Olabi, 1994; Olabi and Hashmi, 1996). Channels of different geometries were opened on its surface in order to evaluate the changes induced by curvature. The rectangular channels serve as a reference for comparison to the semicircular channels. The cylindrical profiles, referred as 1, 2 and 3, have diameters of 3, 6, and 10 mm respectively, while the flat grooves (A, B, and C) have respective dimensions of 4x1, 7x2, and 10x4 mm. The positioning of the channels is such that every groove is placed in the middle of its two opposites, so that the machining of one face of the block does not affect the other. The smaller diameter was chosen in order to correspond to the 1/3 surface-to-collimator ratio determined by Oguri *et al.* as the limiting condition for significant errors due to curvature. Measurement of the dimensions of each groove showed adequate concordance with those initially desired.

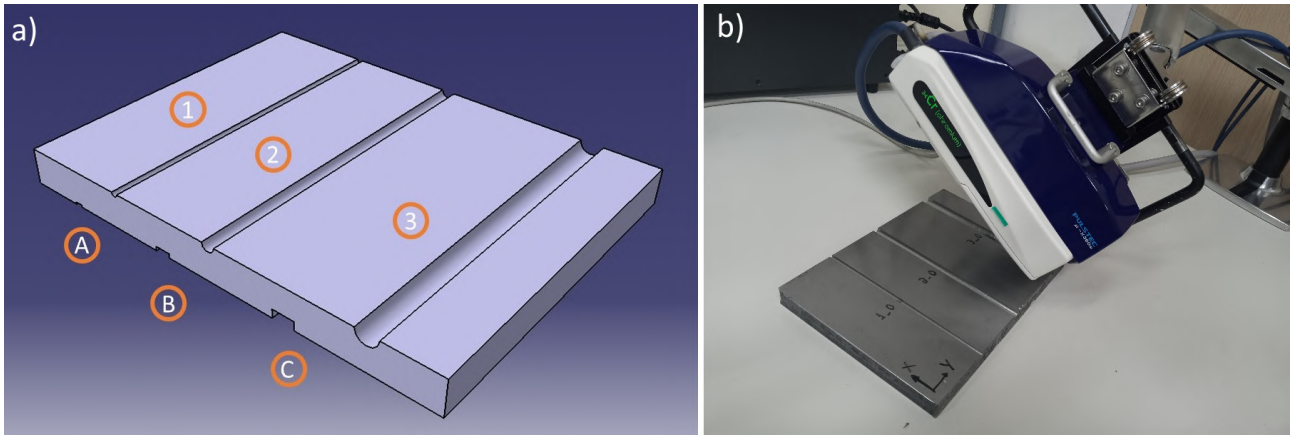

Figure 1. a) Geometry of the specimen employed in curvature influence analysis, and b) residual stress measurement being performed on the specimen.

The comparison of groove geometries is only valid if the induced stress state before measurement is similar for every channel. The residual stress after grinding was measured at nine equally spaced points on each side of the block, confirming it to be initially homogeneous. As a measure of controlling the surface conditions after milling of the channels, the material removal rate (MRR) was fixed for every indented groove, being given for a cut with constant A_0 area by:

$$MRR = A_0 \cdot f, \tag{1}$$

where f is the feed rate. The areas of the rectangular sections were chosen as to be similar to the semicircular ones. Thus, by fixing the feed rate and achieving approximately the same material removal rate for all channels, similar stress states should be induced (Capello, 2005; Jiang *et al.*, 2013).

The machining of the grooves utilized a ROMI DCM 620-5X CNC machine at a constant 200 mm/min feed rate and at 2000 rpm tool speed for every channel. A, B and C were cut at two steps of 0.5 mm, two steps of 1 mm, and four of 1 mm, respectively. Channels 1, 2 and 3 were respectively milled at five steps of 0.3 mm, three of 1 mm, and four steps at 1.5, 3, 4 and 5 mm of depth. All tools used, detailed on Tab. 2, were either new or had light wear, such that their condition is unlikely to have significantly affected the machining results.

Table 2. Tools used for machining of the grooves.

Groove	Diameter (mm)	Tool
A	4	ISCAR cylindrical end mill, three flutes
B	7	YG1 coated carbide G9424070 cylindrical end mill, two flutes
C	10	HT TiAlN DIN6527 cylindrical end mill, two flutes
1	3	SANDVIK R216,42-03030-Al03T 1620 ball end mill, two flutes
2	6	SANDVIK R216,42-06030-AC10P 1620 ball end mill, two flutes
3	10	YG1 coated carbide G9624100 ball end mill, two flutes

A point was marked at half the length of each channel, being named 1_0, 2_0 and 3_0 for the cylindrical grooves, and A_0, B_0 and C_0 for the rectangular ones. Residual stresses were then measured ten times on every point and for

each direction (radial and circumferential), as also depicted in Fig. 1. Subsequently, in order to verify possibly non-representative stress state conditions at the points evaluated, as well as to further diminish errors due to positioning, ten points were marked along the length of every channel, and residual stresses were measured once for each direction on every point.

2.2 Gear teeth analysis

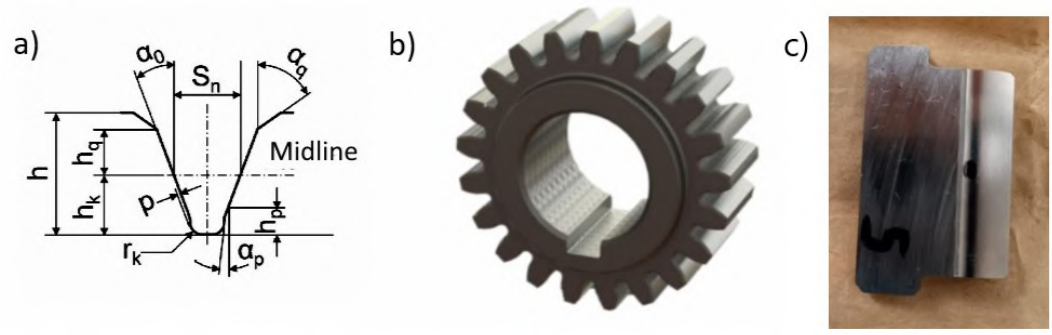

Figure 2. a) Specification of the parameters considered for the ITA geometry tooth profile, b) 3D drawing of an ITA geometry gear, and c) a sectioned gear tooth.

Five teeth of a case hardened AISI 4320 gear were analyzed on a single point at the middle of their root channels and on five points across each of them, generating results compatible with real gear analysis procedures. The tooth profile parameters of the gears employed in the experiments are specified in Fig. 2, and its corresponding geometric dimensions are shown on Tab. 3.

Table 3. Dimensions of the tooth profile of the gears analyzed, as shown in Fig. 2.

Dimension	Value
a_0	17.5°
a_p	0.0°
a_q	0.0°
h	8.056 mm
h_k	3.234 mm
h_p	0.0 mm
h_q	4.822 mm
p	0,0 mm
r_k	0.570 mm

The S_n parameter, corresponding to the distance between two teeth at the midline, was not specified in the profile, but measured with a Mitutoyo CD-6 ASX-B vernier caliper on three gears of ITA geometry. A value of 3.61 ± 0.05 mm at 95% confidence level was obtained with 10 measurements for each gear done on different pairs of teeth.

It should be noted that the collimator diameter, of 1 mm, is greater than a third of the tooth root diameter, of 1.140 mm as specified in the teeth profile. Therefore, if the 1/3 ratio limit is applicable to concave surfaces, the error introduced by curvature should be significant for the gears analyzed.

3. RESULTS AND DISCUSSION

A schematic of the axes considered in the geometry analyses is shown in Fig. 3, where x denotes the axial direction and y the circumferential direction.

3.1 Specimen analysis

For reference, the residual stress was at first measured for both directions on the plane top surface at six points, each of them close to a specific groove. These results are shown on Fig. 4, where it can be seen that, on the surface, the residual stresses are close to null at each point.

Residual stress measurements on the y direction for every curved groove and for the flat channel with the greatest diameter generated incomplete, undesirable Debye-Scherrer rings as shown in Fig. 5, since local inclination causes diffracted X-rays to be detected at incorrect spots. Since groove C is deeper than B and A, a larger ”shadow" is cast by

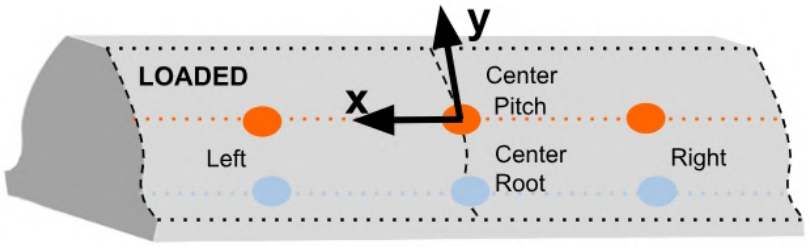

Figure 3. Schematic of the tooth geometry considered in the residual stress measurements.

its walls onto it, preventing some X-rays to penetrate and return, which is the reason for the subpar Debye-Scherrer rings generated for that groove in particular. Without further processing, these results do not describe a coherent residual stress pattern at the point evaluated, and cannot be considered valid.

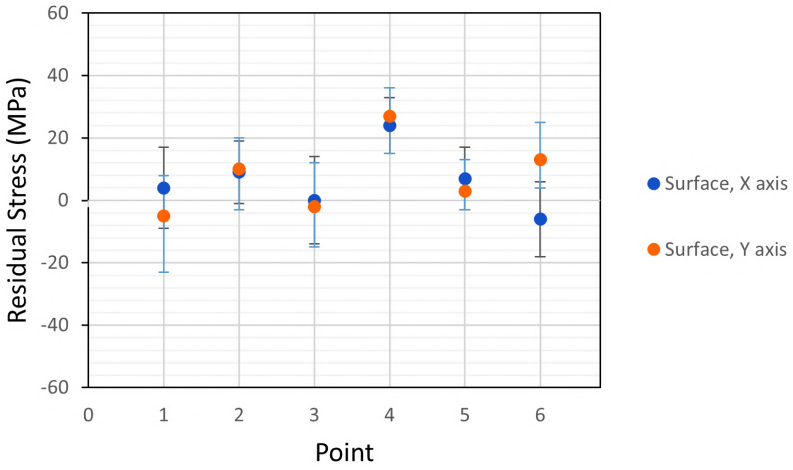

Figure 4. Residual stress measurements for the x and y directions on the surface of the specimen, at six different points.

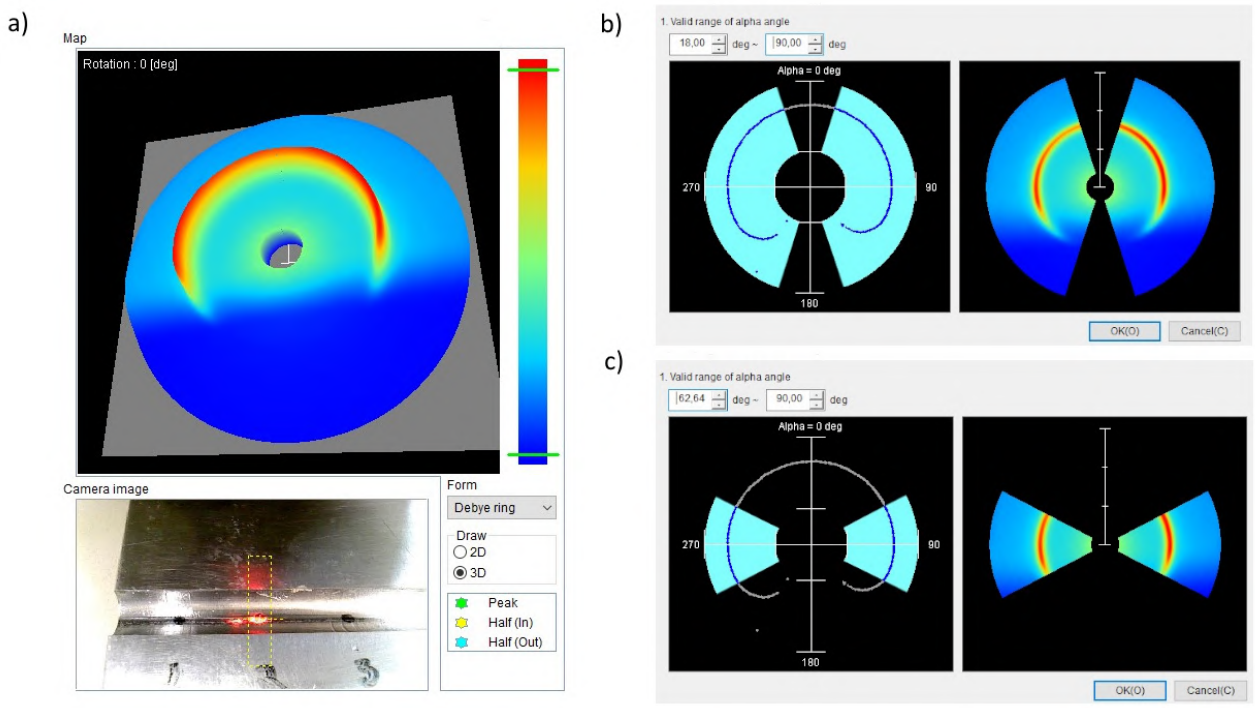

Figure 5. a) Example of an undesirable Debye-Scherrer ring obtained, and its α angle range parameter: b) before (using default parameters), and c) after redefinition.

In order to generate valid results, the α angle analysis range was redefined for every measurement that featured a subpar Debye-Scherrer ring, such that only regions with coherent residual stress conditions were considered. Since calculations via the cosα method involve differences between diametrically opposite points on the ring, if one of them is discarded, its opposite must also be necessarily disregarded. Although loss of information is inevitable with the use of such tool, it is necessary to ensure reasonable stress values are obtained, which can be accurately used to assess the true condition of the region evaluated. Range redefinition was employed for every curved channel and for the C groove on their y direction measurements, and it was not needed for any x axis measurements.

The residual stress evaluation results for the curved channels are compared for both axes on Fig. 6. It can be observed that measurements along the axial direction were more precise than those in the circumferential direction for both the same point measurements and those done throughout the channels. Groove 1 (with the smallest diameter) exhibited the highest deviations, which can be explained by its smaller diameter causing higher local inclination and, consequently, more significant measurement error. This behavior indicates the existence of a significant influence of the curvature on the residual stress results found, since it is expected that groove 1 would have a similar residual stress state of the other two channels, considering the specimen underwent stress relief heat treatment. This result seems to agree with the observations of Oguri *et al.* in that only the groove with the curvature smaller than 1/3 of the equipment's collimator showed significant disparity from the expected value. However, the residual stress values found for groove 1 were more compressive than for the other curved channels, a behavior opposite to that observed by the researchers on their experiments. A similar behavior is observed for the single point and multiple point measurements, though grooves 2 and 3 are less homogeneous in the latter.

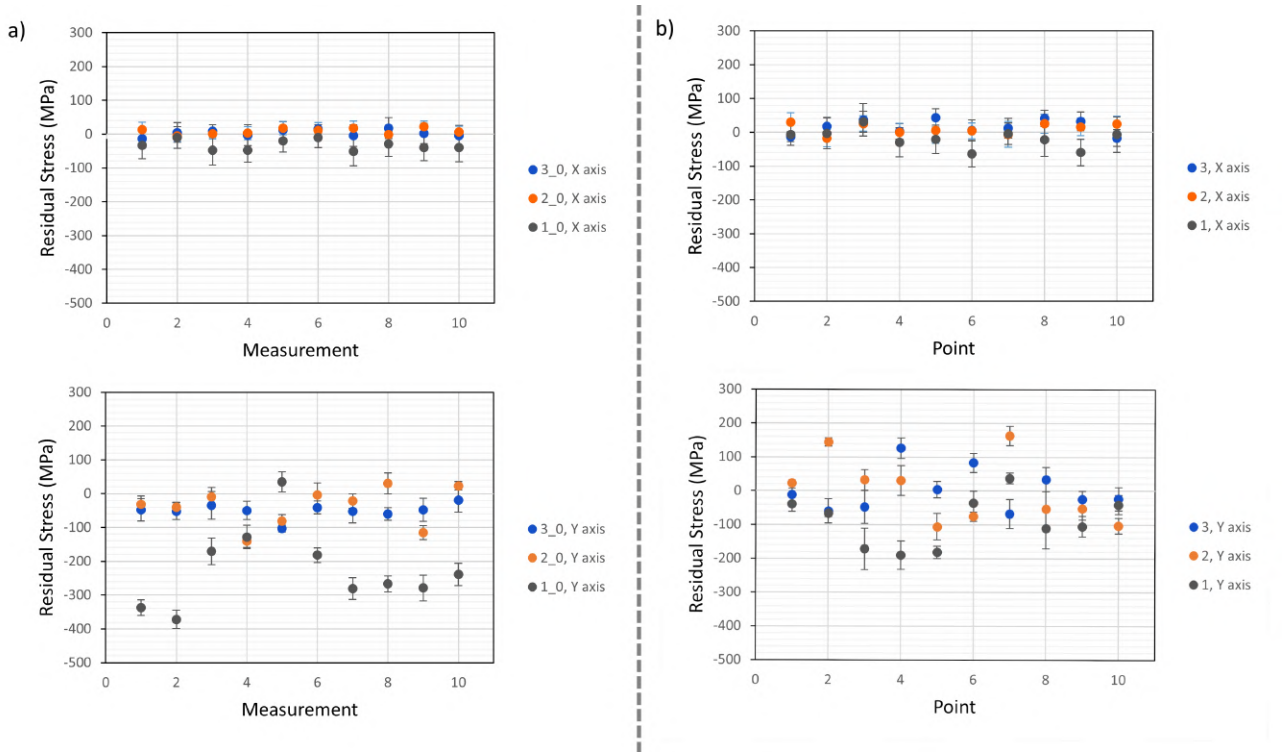

Figure 6. Residual stress results for channels 1, 2 and 3 along the x and y directions, for: a) their midpoints, and b) across their length.

A comparison between the cylindrical and rectangular channels is shown in Fig. 7. It can be observed that even residual stresses measured on the y direction for the flat grooves were close to null, a behavior not shared by the curved surface with the smallest diameter and partially by grooves 2 and 3, which did show higher deviations on their y axis measurements but not as significantly as groove 1. Again, behaviors were similar for single and multiple point measurements, with slight higher homogeneity of residual stresses on groove 1 in the latter.

The difference in results for flat and curved grooves without material rate fixing and stress relief treatment would occur mainly due to disparity of the residual stress state induced by their machining, which can be caused by factors such as different heat transfer between tool and surface or altered plastic interactions due to geometry. Once these influences were diminished by stress relief, it can be observed from the axial direction results and the circumferential ones for higher diameter grooves that the rectangular and cylindrical channels reached very similar, low magnitude residual stress states. Therefore, it is reasonable to conclude that the main influence for residual stress disparity on groove 1 was, in fact, its higher curvature.

From the experiments carried out, it can safely be assumed that the axial measurements were accurate regardless of groove curvature, and that analysis in this direction can be performed on small diameter surfaces such as gear teeth roots without significant errors in precision or accuracy due to the curvature effect. The circumferential measurements can also be assumed to be accurate for sufficiently high diameter surfaces, although α angle range redefinition can be necessary to limit stress calculations to valid regions of the Debye-Scherrer ring.

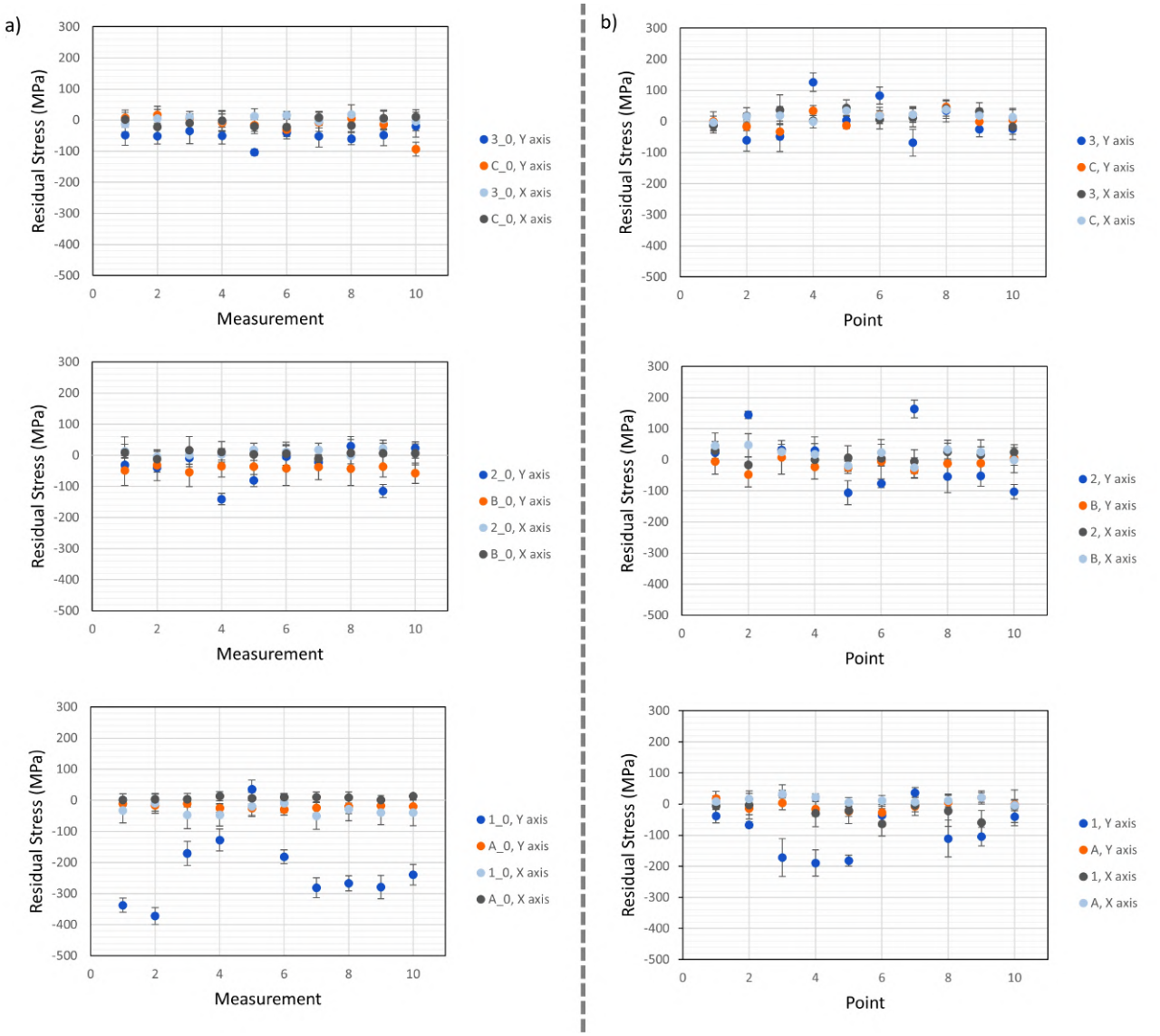

Figure 7. Residual stress comparison in the x and y directions between channels 3 and C, 2 and B, and 1 and A, for: a) their midpoints, and b) across their length.

3.2 Gear teeth analysis

For reference, residual stress measurements were done at the midpoint of each tooth flank, on both the axial and circumferential directions. These results are shown on Fig. 8. The residual stress measurements for the root regions of an ITA geometry AISI 4320 gear's teeth are shown on Fig. 9.

It can be observed that x direction measurements for the gear teeth roots were not more precise than those in the y direction, being in fact slightly less precise. This result, at first, seems to contradict previous research and the conclusions derived from the specimen analysis, since the circumferential direction should exhibit more deviation due to the greater curvature influence, especially at a small diameter region such as the tooth root.

One explanation for this behavior would be that the root region is so narrow that the refracted X-rays collected come mainly from flank area. However, considering that the residual stress measurements for the tooth flanks are significantly more compressive than those obtained from the root measurements, a higher influence of the flank area should result in more compressive residual stress states than those observed, which does not happen.

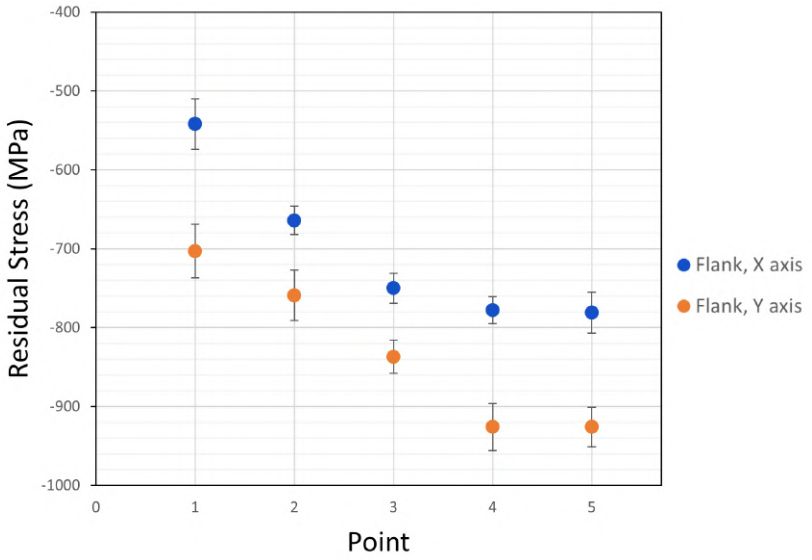

Figure 8. Residual stress measurements for each tooth flank on the x and y directions.

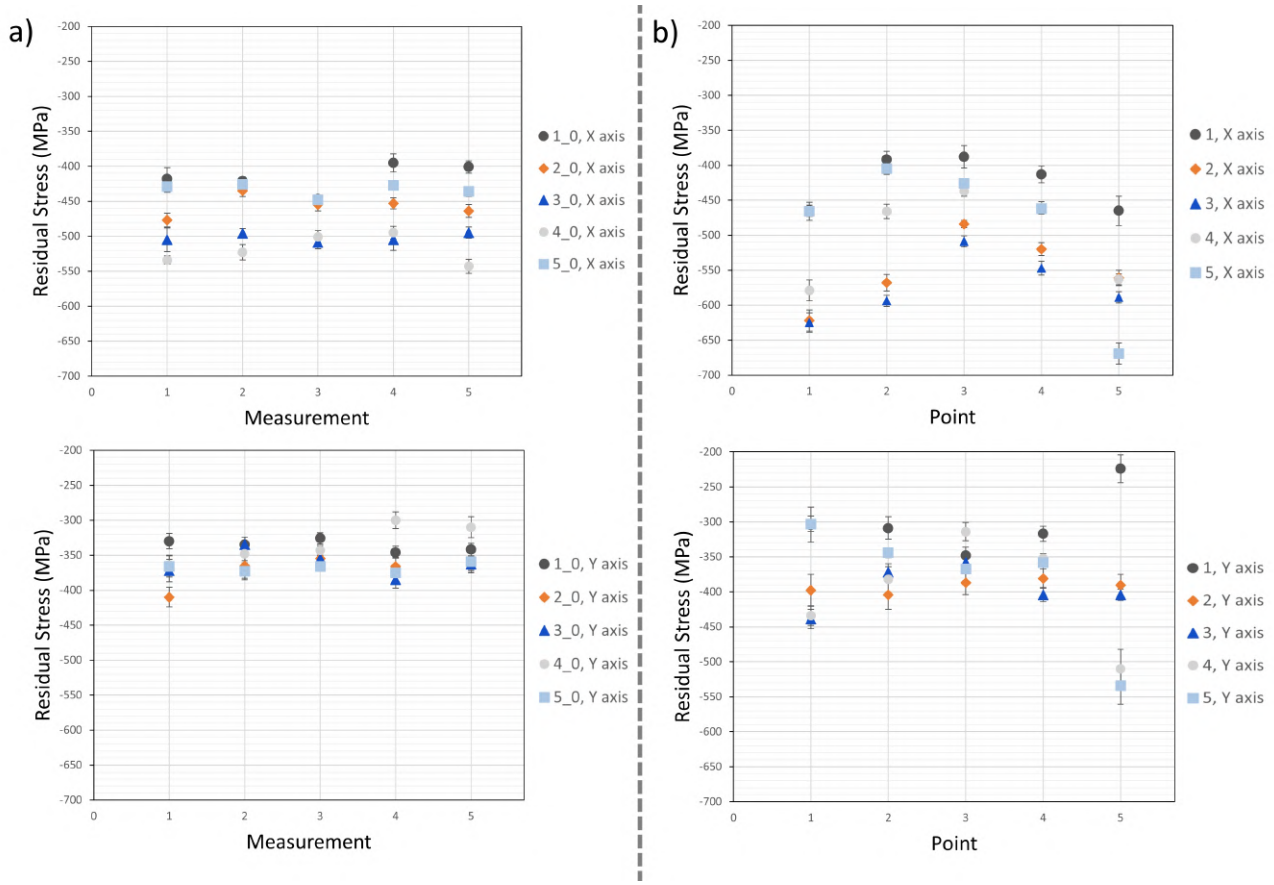

Figure 9. Residual stress results for five case hardened ITA geometry gear teeth: a) at their midpoints, and b) across their length.

Another explanation for this apparent contradiction is that the X-rays were cast not only to the small radius section of the root region, but also to its uppermost part, as represented on Fig. 10. This area, when measured, would show less influence from curvature effects, since it is significantly more leveled.

If evaluation of the entire tooth root area is desired, given the results found, the cosα X-ray diffraction technique can be employed in order to generate precise results for both axial and circumferential directions. However, the crack nucleation of most tooth bending fatigue failures occurs at the small radius root region (Kale, 2013), subjected to the greatest tensile stress during operation, such that it is of interest to evaluate the residual stress state at this specific area.

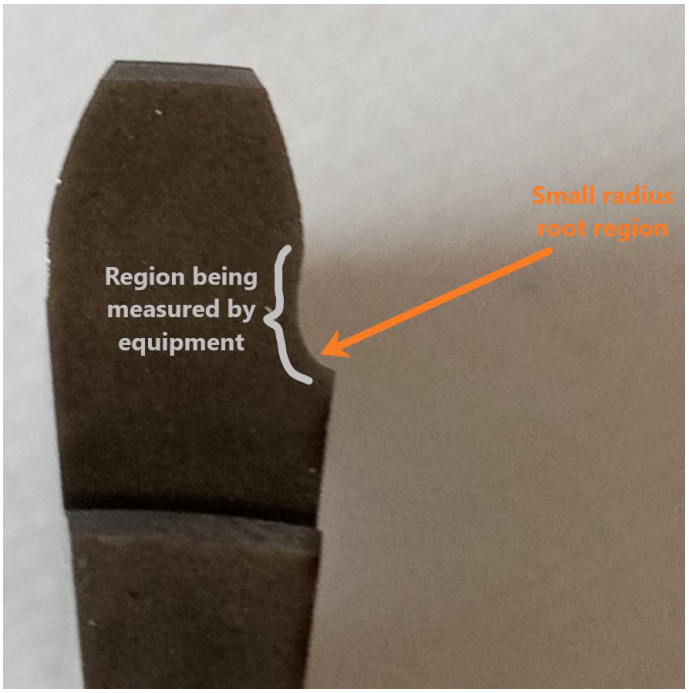

Figure 10. Different root regions for the analyzed gear teeth.

If this hypothesis is correct, it can be concluded that, in order to properly assess the gear's residual stress state at the root region, modifications are needed in the procedure, such that the measurement method cannot be the same as for the flank area. A way to possibly mitigate this problem is to cover with tape parts of the tooth whose measurement is not desired so as to eliminate their influence, although presumably with great loss of information and generation of suboptimal Debye-Scherrer rings. Other tooth sectioning methods can also be explored in order to further expose the root region for residual stress measurements, as well as the utilization of smaller collimators, if available.

4. CONCLUSIONS

Residual stress measurements using the cosα X-ray diffraction technique on rectangular and cylindrical channels indented on a ground and stress relieved steel block showed a high level of precision achieved for the axial direction regardless of curvature. The values for the circumferential direction on the curved grooves were accurate for those with the largest diameters (from 6 to 10 times bigger than that of the equipment's collimator), after α angle range redefinition was employed to limit the residual stress calculations exclusively to valid regions of the Debye-Scherrer rings. Disparity in results was significantly larger on the curved groove with the smallest diameter (3 times larger than the collimator's) along the circumferential axis, suggesting a strong influence of curvature.

At the root region of different gear teeth, residual stress measurements were precise for both directions, suggesting the absence of curvature influence. This can be explained by the casting of most X-rays onto the surface immediately above the root region with the smallest radius, which is significantly less curved. Since the smallest radius root area is the most important for evaluation of tooth bending fatigue, modifications are necessary in the standard cosα X-ray diffraction measurement procedure, such as covering with tape the regions of the tooth whose residual stress assessment is not necessary.

To further validate the employment of cosα X-ray diffraction at the tooth root, an immediate next step in this research is to verify the efficiency of the proposed alternative measurement technique. For additional improvement of residual stress measurements at the gear tooth root, more factors should be taken into consideration, such as the optimal setting of equipment parameters and the microstructure of the regions analyzed. An improved understanding of how to properly evaluate the residual stress state at the root region in gears is important to raise their fatigue limits, prevent premature failures and create overall better components.

5. ACKNOWLEDGMENTS

The authors gratefully acknowledge the support of the Casimiro Montenegro Filho Foundation (FCMF) and of the Competence Center in Manufacturing of the Aeronautics Institute of Technology (CCM-ITA), where the research was conducted.

6. REFERENCES

Alban, L.E., 1985. *Systematic Analysis of Gear Failures*. American Society for Metals, Ohio, 3rd edition.

Capello, E., 2005. "Residual stresses in turning: Part i: Influence of process parameters". *Journal of Materials Processing Technology*, Vol. 160, No. 2, pp. 221–228.

James, M., Hughes, D., Chen, Z., Lombard, H., Hattingh, D., Asquith, D., Yates, J. and Webster, P., 2007. "Residual stresses and fatigue performance". *Engineering Failure Analysis*, Vol. 14, No. 2, pp. 384–395. Papers presented at the 22nd meeting of the Spanish Fracture Group (Almargro, Spain, March 2005).

Jiang, X., Li, B., Yang, J. and Zuo, X.Y., 2013. "Effects of tool diameters on the residual stress and distortion induced by milling of thin-walled part". *The International Journal of Advanced Manufacturing Technology*, Vol. 68, No. 1, pp. 175–186.

Kale, A.S., 2013. "Bending fatigue failure in gear tooth". *International Journal of Engineering Research Technology*, Vol. 02.

Kramberger, J., Šraml, M., Glodež, S., Flašker, J. and Potrč, I., 2004. "Computational model for the analysis of bending fatigue in gears". *Computers Structures*, Vol. 82, No. 23, pp. 2261–2269. Computational Structures Technology.

Nelson, D., 1982. "Effects of residual stress on fatigue crack propagation". pp. 172–174.

Oguri, T., Tanaka, T., Okano, T., Murata, K., Kawakami, H. and Sato, Y., 2017. "X-ray stress measurement of the cylindrical surface by the cosα method". *Journal of the Society of Materials Science, Japan*, Vol. 66, pp. 488–494.

Olabi, A., 1994. *Residual stresses and heat treatments for metallic welded components*. Ph.D. thesis, School of Mechanical and Manufacturing Engineering, Dublin City University.

Olabi, A. and Hashmi, M., 1996. "Stress relief procedures for low carbon steel (1020) welded components". *Journal of Materials Processing Technology*, Vol. 56, No. 1, pp. 552–562. International Conference on Advances in Material and Processing Technologies.

Peterson, N., Kobayashi, Y., Traeger, B. and Sanders, P., 2017. "Assessment and validation of cosα method for residual stress measurement". *Proceedings of the ICSP13*, pp. 80–86.

Tanaka, K., 2018. "X-ray measurement of triaxial residual stress on machined surfaces by the cosα method using a two-dimensional detector". *Journal of Applied Crystallography*, Vol. 51, No. 5, pp. 1329–1338.

7. RESPONSIBILITY NOTICE

The authors are solely responsible for the printed material included in this paper.